Alzheimer's Research & Therapy

RESEARCH

Open Access

Different associations between amyloid-βeta 42, amyloid-βeta 40, and amyloid-βeta 42/40 with soluble phosphorylated-tau and disease burden in Alzheimer's disease: a cerebrospinal fluid and fluorodeoxyglucose-positron emission tomography study

Caterina Motta[1*], Martina Gaia Di Donna[1], Chiara Giuseppina Bonomi[1], Martina Assogna[1,2], Agostino Chiaravalloti[3,4], Nicola Biagio Mercuri[1], Giacomo Koch[2,5] and Alessandro Martorana[1]

Abstract

Background Despite the high sensitivity of cerebrospinal fluid (CSF) amyloid beta $(A\beta)_{42}$ to detect amyloid pathology, the $A\beta_{42}/A\beta_{40}$ ratio (amyR) better estimates amyloid load, with higher specificity for Alzheimer's disease (AD). However, whether $A\beta_{42}$ and amyR have different meanings and whether $A\beta_{40}$ represents more than an $A\beta_{42}$-corrective factor remain to be clarified. Our study aimed to compare the ability of $A\beta_{42}$ and amyR to detect AD pathology in terms of p-tau/$A\beta_{42}$ ratio and brain glucose metabolic patterns using fluorodeoxyglucose-positron emission tomography (FDG-PET).

Methods CSF biomarkers were analyzed with EUROIMMUN ELISA. We included 163 patients showing pathological CSF $A\beta_{42}$ and normal p-tau (A+T− =98) or pathological p-tau levels (A+T+ =65) and 36 control subjects (A−T−). A+T− patients were further stratified into those with normal ($CSFA\beta_{42}$+/amyR− =46) and pathological amyR ($CSFA\beta_{42}$+/amyR+ =52). We used two distinct cut-offs to determine pathological values of p-tau/$A\beta_{42}$: (1) ≥ 0.086 and (2) ≥ 0.122. FDG-PET patterns were evaluated in a subsample of patients (n =46) and compared to 24 controls.

Results CSF $A\beta_{40}$ levels were the lowest in A−T− and in $CSFA\beta_{42}$+/amyR−, higher in $CSFA\beta_{42}$+/amyR+ and highest in A+T+ (F =50.75; p <0.001), resembling CSF levels of p-tau (F =192; p <0.001). We found a positive association between $A\beta_{40}$ and p-tau in A−T− (β =0.58; p <0.001), $CSFA\beta_{42}$+/amyR− (β =0.47; p <0.001), and $CSFA\beta_{42}$+/amyR+ patients (β =0.48; p <0.001) but not in A+T+. Investigating biomarker changes as a function of amyR, we observed a weak variation in CSF p-tau (+2 z-scores) and $A\beta_{40}$ (+0.8 z-scores) in the normal amyR range, becoming steeper over the pathological threshold of amyR (p-tau: +5 z-scores, $A\beta_{40}$: +4.5 z-score). $CSFA\beta_{42}$+/amyR+ patients showed a significantly higher probability of having pathological p-tau/$A\beta_{42}$ than $CSFA\beta_{42}$+/amyR− (cut-off ≥ 0.086: OR 23.3; cut-off ≥ 0.122: OR 8.8), which however still showed pathological values of p-tau/$A\beta_{42}$ in some cases (cut-off ≥ 0.086: 35.7%; cut-off ≥ 0.122: 17.3%) unlike A−T−. Accordingly, we found reduced FDG metabolism

*Correspondence:
Caterina Motta
caterinamotta86@hotmail.it
Full list of author information is available at the end of the article

in the temporoparietal regions of CSFAβ_{42}+/amyR− compared to controls, and further reduction in frontal areas in CSFAβ_{42}+/amyR+, like in A+T+.

Conclusions Pathological p-tau/Aβ_{42} and FDG hypometabolism typical of AD can be found in patients with decreased CSF Aβ_{42} levels alone. AmyR positivity, associated with higher Aβ_{40} levels, is accompanied by higher CSF p-tau and widespread FDG hypometabolism.

Keywords Alzheimer's disease, Cerebrospinal fluid biomarkers, Amyloid beta 40, Amyloid beta 42, Amyloid beta 42/40 ratio, Phosphorylated-tau, Fluorodeoxyglucose-positron emission tomography

Background

According to the amyloid cascade hypothesis, Alzheimer's disease (AD) develops due to amyloid peptides (Aβ) deposition in senile plaques, followed by the accumulation of hyperphosphorylated tau proteins (p-tau) in tangles, ultimately leading to neuronal degeneration and cognitive decline. In 2018, the National Institute on Aging-Alzheimer's Association (NIA-AA) reported that the highest probability of identifying AD pathology in vivo is achieved by combining markers of Aβ (A) and p-tau (T) pathology [1]. Indeed, it has been demonstrated that the co-presence of A+ and T+ status, as well as combining them in the CSF p-tau/Aβ_{42} ratio, provides excellent predictive power for the presence of AD pathology at autopsy [2, 3]. However, when there is no concordance between A and T, and notably when the CSF levels of Aβ_{42} are abnormal (A+) without concomitant abnormal values of p-tau (T−), we encounter an ambiguous biological profile, labeled "AD pathological changes," which is still considered part of the Alzheimer's continuum. Given the crucial role of the "A" status in this biological condition, inconsistencies among different amyloid biomarkers, from cerebrospinal fluid (CSF) or imaging, can represent a significant limitation in supporting a possible diagnosis of AD, thus fueling the need to improve their accuracy.

In this regard, it has been demonstrated that the addition of CSF Aβ_{40} to CSF Aβ_{42} levels in the Aβ_{42}/Aβ_{40} ratio (amyR) could account for inter-individual variations in Aβ production, thereby enhancing the diagnostic performance of this biomarker [4–8]. Furthermore, amyR seems to better reflect the total amount of amyloid brain deposition [9–12]. Nevertheless, Vromen and colleagues also found that the decrease of CSF Aβ_{42} alone shows excellent accuracy in detecting autopsy-confirmed AD [13]. Together, these data support the idea that amyR and Aβ_{42} may provide different kinds of information on the underlying AD pathophysiology.

In the present study, we aimed to determine whether CSF Aβ_{40} has a specific meaning, which enables amyR to better estimate the AD-related burden, and whether pathological CSF Aβ_{42} in the presence of normal amyR can still identify AD pathology. To address this issue, we focused on the A+T− biological condition, stratifying patients with decreased CSF Aβ_{42} into those with normal (CSFAβ_{42}+/amyR−) or pathological amyR (CSFAβ_{42}+/amyR+). We assessed differences and overlaps with healthy control subjects (A−T−) and full-blown AD patients (A+T+) in terms of disease burden measured as CSF p-tau/Aβ_{42} [2, 14] and cerebral glucose hypometabolism, evaluated with fluorodeoxyglucose-positron emission tomography (FDG-PET), whose specific topographical patterns have achieved an increasingly supportive role in the diagnostic algorithm of AD [15–17].

Materials and methods

Subjects' enrolment

Between 2017 and 2021, we evaluated 250 patients at the Memory Clinic of the "Policlinico Tor Vergata" in Rome. The criteria for retrospective inclusion were as follows: (1) a complete diagnostic workup, including standardized neurological examination, laboratory testing, MRI imaging, FDG-PET scan, neuropsychological assessment, APOE genotyping, and CSF analysis, and (2) fulfillment of the diagnostic criteria for dementia [18] or mild cognitive impairment due to AD [19]. Exclusion criteria were as follows: (1) presence of other neurological or psychiatric diseases or medical conditions potentially associated with cognitive deficits; (2) major comorbidities such as oncological history, systemic inflammatory conditions, and organ failure; (3) prominent cortical or subcortical infarcts; (4) history of drug or alcohol abuse; (5) use of antipsychotics, antidepressants, or serotonergic drugs.

Eventually, we selected 163 patients belonging to the Alzheimer's continuum (ADc) according to their biomarker profile [1]. Further stratification into AT groups was performed according to the presence of decreased CSF levels of Aβ_{42} (A) and increased CSF p-tau (T) (see Additional file 1).

Furthermore, we identified 36 controls among inpatients from the Neurology Unit of Policlinico Tor Vergata who had undergone a complete neurological evaluation, brain CT, and lumbar puncture for diagnostic purposes and for which the presence of any primary neurological disease had been excluded. All CSF analyses showed normal cell counts and biomarker profiles.

CSF sampling/analysis and APOE genotyping

All lumbar punctures were performed between 8 and 10 am. An 8 ml CSF sample was collected for each patient in polypropylene tubes, 2 ml were used for routine biochemical analysis, 6 ml were centrifuged at 2000 g at + 4 °C for 10 min, and frozen at − 80 °C. All samples were processed according to the manufacturer's instructions and to laboratory standard operating procedures.

The levels of CSF $A\beta_{42}$ and $A\beta_{40}$, t-tau, and p-tau phosphorylated at Thr181 (p-tau181) were determined using a sandwich enzyme-linked immunosorbent assay (EUROIMMUN ELISA©). The cut-off values for CSF $A\beta_{42}$, CSF p-tau, and CSF t-tau were determined following EUROIMMUN guidelines: CSF $A\beta_{42} > 600$ pg/ml, CSF amyR > 0.06, CSF p-tau < 65 pg/ml, CSF t-tau < 400 pg/ml. Given the absence of manufacturer's guidelines for the p-tau/$A\beta_{42}$ cut-off and of neuropathological/amyloid PET imaging validation in literature, we performed our analyses on AD-related burden (p-tau/$A\beta_{42}$) considering two separate thresholds to determine pathological values: (1) ≥ 0.086, determined with a similar ELISA technique (INNOTEST©) and validated on neuropathological data [2], and (2) ≥ 0.122, determined on EUROIMMUN assays with a Youden Index analysis to discriminate between biologically defined AD and non-AD patients [20].

APOE genotyping was performed using allelic discrimination technology with real-time PCR (TaqMan; Applied Biosystems). Patients were classified as APOE4 when carrying either one (APOE ε3/ε4) or two (APOE ε4/ε4) ε4 alleles. All the remaining patients were identified as APOE3 (ε3/ε3).

FDG-PET substudy

Study population

The study was conducted at the Nuclear Medicine Unit of Policlinico Tor Vergata in Rome (General Electric VCT PET/CT scanner). Among the enrolled patients, 46 had undergone FDG-PET at our site (CSFAβ42 + /amyR − , $n = 9$; CSFAβ42 + /amyR + , $n = 17$; A + T + , $n = 20$).

Moreover, 24 subjects (male, 10; female, 14; mean age, 66.56 ± 10.44 years) undergoing FDG-PET/CT for other reasons were enrolled as part of a control group (CG) upon showing no signs of hypometabolism suggestive of neurodegenerative disorders nor other cerebral abnormalities, as assessed by visual reads (A.C). All subjects had an MRI performed within 14 ± 4 days before PET/CT examination, showing absence of brain alterations. An experienced neurologist (A.M.) evaluated all participants to assess the absence of clinical signs of cognitive decline. Patient and control selection strategies for the sub-study are summarized in Additional file 2.

FDG-PET/CT scanning and acquisition

The same scanning and acquisition protocol was used for both patients and CG. All subjects were injected with intravenous FDG (dose range 185–295 megabecquerels) and hydrated with 500 ml of saline (0.9% sodium chloride). PET/CT acquisition started 30 ± 5 min after FDG injection and lasted for 10 min in all subjects. The reconstruction parameters were as follows: ordered subset expectation maximization, four subsets and 12 iterations; matrix 256 × 256; full width at half maximum (FWHM): 5 mm.

Data management and statistical analysis

CSF biomarkers analysis

All continuous variables were expressed as mean ± standard deviation. The Kruskal–Wallis test and Dunn's post hoc analysis were used for multiple comparisons. Categorical variables were analyzed using Pearson's chi-square test. We computed a linear regression model with age and sex as covariates to study the association between CSF amyloid biomarkers and CSF p-tau levels. We then performed a robust locally weighted regression analysis [21] and plotted CSF biomarkers levels as a function of amyR, using CSF biomarkers values converted to z-scores by subtracting the mean and dividing by the standard deviation of the control group (A − T −). Eventually, logistic multivariate regressions were performed to evaluate the odds of pathological p-tau/$A\beta_{42}$ values according to amyR status, accounting for clinical and demographic factors (age, sex, APOE, diabetes mellitus, hypertension, dyslipidemia).

All statistical analyses were performed using StataCorp© (Stata Statistical Software: Release 13. College Station, TX: StataCorp) and GraphPad Prism version 9.3.1 (GraphPad Software, San Diego, California, USA). All results were computed with two-tailed significance; $p < 0.05$ were considered significant.

FDG-PET analysis

First, all FDG-PET scans were visually evaluated in standardized transaxial, coronal, and sagittal plans by an experienced nuclear medicine physician (A.C) and interpreted according to the latest EANM guidelines for FDG-PET imaging [22]. We used Statistical Parametric Mapping 12 (SPM12) in MATLAB 2018a (https://www.fil.ion.ucl.ac.uk/spm/software/spm12/) to perform statistical analysis. FDG-PET data were converted from DICOM to Nifti format using Mricron software (https://www.nitrc.org/projects/mricron) and then subjected to a normalization process. A bias regularization was applied (0.0001) to limit biases due to smoothness, spatially varying artifacts that modulate the intensity of

the image and that can impede automating processing of images. FWHM of Gaussian smoothness of bias (to prevent the algorithm from trying to model out intensity variation due to different tissue types) was set at 60 mm cut-off; tissue probability map implemented in SPM12 was used (TPM.nii). A mutual information affine registration with the tissue probability maps [23] was used to achieve approximate alignment to ICBM space template—European brains [24, 25]. Warping regularization was set with the following 1 by 5 array (0, 0.001, 0.5, 0.05, 0.2); smoothness (to cope with functional anatomical variability that is not compensated by spatial normalization and to improve the signal-to-noise ratio) was set at 5 mm; sampling distance (that encodes the approximate distance between sampled points when estimating the model parameters) was set at 3. We applied an 8-mm isotropic Gaussian filter to blur the individual variations (especially gyral variations) and to increase the signal-to-noise ratio. We used the following parameters and post-processing tools before regression analysis was applied: global normalization (that scales images to a global value) = 50 (using proportional scaling); masking threshold (that helps to identify voxels with an acceptable signal in them) was set to 0.8; transformation tool of statistical parametric maps into normal distribution; correction of SPM coordinates to match the Talairach coordinates, subroutine implemented by Matthew Brett (http://www.mrc-cbu.cam.ac.uk/Imaging). Brodmann areas (BA) were identified at a range from 0 to 3 mm from the corrected Talairach coordinates of the SPM output isocenter, using a Talairach client available at http://www.talairach.org/index.html. As proposed by Bennett et al. [26], SPM t-maps were corrected for multiple comparisons using the false discovery rate ($p \leq 0.05$) and corrected for multiple comparisons at the cluster level ($p \leq 0.001$). The level of significance was set at 100 contiguous voxels (5 × 5 × 5 voxels, i.e., 11 × 11 × 11 mm). The following voxel-based comparisons were assessed: CG vs. $CSFA\beta_{42}+$/amyR−, $CSFA\beta_{42}+$/amyR− vs. $CSFA\beta_{42}+$/amyR+, and $CSFA\beta_{42}+$/amyR+ vs. A+T+. We used a full factorial design implemented in SPM12 to test the hypothesis that differences among groups exist overall. Comparisons between groups were performed using the two-sample *t*-test model of SPM12. For both analyses, age and sex were used as covariates, and the threshold was set at $p < 0.001$ ($p < 0.05$ FWE corrected at the cluster level).

Results

Participants' selection and characteristics

From 250 subjects with suspected AD-related cognitive impairment, we enrolled 163 patients with decreased CSF levels of $A\beta_{42}$ and normal CSF p-tau (A+T− = 98) or pathological CSF p-tau (A+T+ = 65), as well as 36 sex-/age-matched healthy controls (A−T−) (see Additional file 1). We further stratified A+T− patients according to the presence of either pathological ($CSFA\beta_{42}+$/amyR+, $n = 46$) or normal amyR ($CSFA\beta_{42}+$/amyR−, $n = 52$). Table 1 shows the clinical and demographic characteristics of the patients according to AT status.

Table 1 Demographic and clinical characteristics across AT groups

	A−T− (*n* = 36)	$CSFA\beta_{42}+$/amyR− (*n* = 52)	$CSFA\beta_{42}+$/amyR+ (*n* = 46)	A+T+ (*n* = 65)	*p*
Age (years)	70.72 ± 3.81	68.90 ± 9.55	71.34 ± 8.91	72.31 ± 6.56	0.15
Male (%)	33.3%	55.7%	60.8%	33.8%	**< 0.01**
CSF $A\beta_{42}$ (pg/ml)	1270.91 ± 196.67	394.45 ± 85.80	341.92 ± 81.18	389.17 ± 105.41	**< 0.001**
CSF $A\beta_{40}$ (pg/ml)	5870.36 ± 1283.07	4740.74 ± 1457.22	8110.55 ± 2490.97	10092.15 ± 3352.14	**< 0.001**
CSF p-tau (pg/ml)	25.27 ± 6.65	29.12 ± 13.63	44.84 ± 13.28	101.37 ± 30.89	**< 0.001**
CSF t-tau (pg/ml)	165.82 ± 60.60	149.30 ± 77.60	233.84 ± 72.53	646.54 ± 261.38	**< 0.001**
CSF p-tau/$A\beta_{42}$	0.02 ± 0.01	0.07 ± 0.04	0.14 ± 0.05	0.28 ± 0.11	**< 0.001**
Qalb	5.62 ± 3.40	8.75 ± 6.33	7.46 ± 4.11	7.44 ± 6.58	**< 0.01**
MMSE	29.19 ± 1.97	21.31 ± 4.82	21.50 ± 5.15	20.25 ± 4.95	**< 0.001**
MCI/Dementia (*n*)	0/0	21/31	18/28	15/50	0.08
Diabetes (%)	38.9%	55.8%	56.5%	58.5%	0.26
Hypertension (%)	47.2%	21.2%	19.6%	15.4%	**< 0.01**
Dyslipidemia (%)	27.8%	19.2%	26.1%	35.4%	0.28
APOE4 (%)	n.a	28.8%	32.6%	55.4%	**< 0.01**

Data are presented as mean ± standard deviation or percentages, when applicable. *CSF* cerebrospinal fluid, *Qalb* albumin quotient, *MMSE* Mini-Mental State Examination, *p p*-value. MMSE score of ≥ 24 was used as a cut-off to separate MCI from dementia patients. Percentages indicate subjects showing the presence of each variable within the group. Bold values represent *p*-value < 0.05

CSF AD biomarkers and disease burden

CSF levels of $A\beta_{42}$ were significantly lower in $CSFA\beta_{42}+$/amyR−, $CSFA\beta_{42}+$/amyR+, and A+T+patients than in A−T−subjects ($F=560.9$; $p<0.001$), but no differences were found among the patient groups ($p>0.05$). Conversely, CSF $A\beta_{40}$ levels were similarly lower in A−T−and $CSFA\beta_{42}+$/amyR−, significantly higher in $CSFA\beta_{42}+$/amyR+, and even higher in A+T+patients ($F=50.75$; $p<0.001$), suggesting that pathological amyR in $CSFA\beta_{42}+$/amyR+and A+T+could be sustained by the concomitant presence of increased $A\beta_{40}$ and decreased $A\beta_{42}$ in the CSF. Similarly, the ANOVA showed lower CSF p-tau levels in A−T−and $CSFA\beta_{42}+$/amyR−, higher in $CSFA\beta_{42}+$/amyR+, and highest in A+T+($F=192$; $p<0.001$).

Finally, p-tau/$A\beta_{42}$ levels were the lowest in A−T−and progressively increased in $CSFA\beta_{42}+$/amyR−, $CSFA\beta_{42}+$/amyR+, and A+T+patients ($F=131.9$; $p<0.001$) (Fig. 1).

Association between amyloid biomarkers and p-tau CSF levels

To explore the association between different CSF amyloid biomarkers ($A\beta_{42}$, $A\beta_{40}$, and amyR) and CSF p-tau levels, we performed correlation (see Additional file 3) and linear regression analyses adjusting for age and sex (see Table 2). $A\beta_{42}$ was associated with p-tau levels only in A−T−subjects ($\beta=0.48$; $p=0.003$), but not in any other AT subgroup. In contrast, a positive association between $A\beta_{40}$ and CSF p-tau levels was found in A−T−($\beta=0.58$; $p<0.001$), $CSFA\beta_{42}+$/amyR−($\beta=0.47$; $p<0.001$), and $CSFA\beta_{42}+$/amyR+patients ($\beta=0.48$; $p<0.001$), but not in A+T+patients. Similarly, amyR was associated with CSF p-tau levels in A−T−($\beta=-0.33$; $p=0.047$), $CSFA\beta_{42}+$/amyR−($\beta=-0.49$; $p<0.001$), and $CSFA\beta_{42}+$/amyR+patients ($\beta=-0.45$; $p<0.001$), but not in A+T+patients.

Given the previous association between amyloid and p-tau markers in the A−T−and A+T−subgroups, we applied a robust locally weighted regression model to trace the trajectories of standardized (z-scores) CSF biomarkers as a function of amyR. We observed that CSF $A\beta_{42}$ dramatically declined, reaching −4.5 *z*-scores, when amyR levels were still normal, and plateaued when amyR became pathological (−5 *z*-scores). Remarkably, CSF $A\beta_{40}$ and p-tau also started to increase before the amyR cut-off was reached (2 *z*-scores for CSF p-tau and 0.8 *z*-scores for $A\beta_{40}$), but steeply increased above the pathological threshold of amyR, eventually reaching the highest z-scores (5 *z*-scores for CSF p-tau and 4.5 *z*-scores for $A\beta_{40}$) (Fig. 2).

Pathological amyR increases odds of pathological p-tau/$A\beta_{42}$ in A+T−

To evaluate the effect of amyR on the AD-related burden, in terms of p-tau/$A\beta_{42}$ ratio, we applied Pearson's

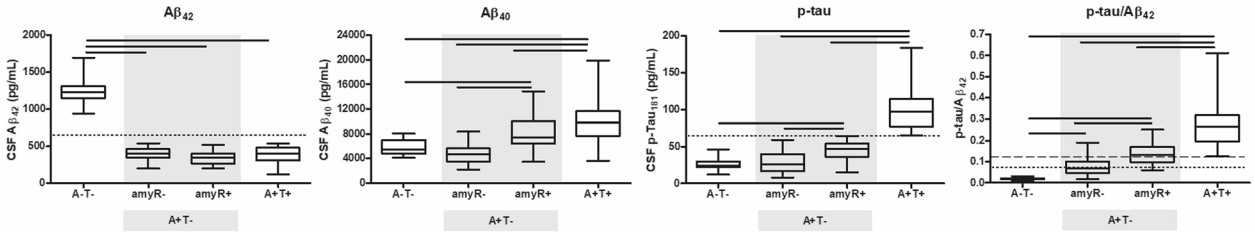

Fig. 1 Intergroup differences of cerebrospinal fluid (CSF) biomarkers. The gray zone includes patients classified as A+T−. Dotted lines represent cut-off values used for $A\beta_{42}$, p-tau, and the p-tau/$A\beta_{42}$ cut-off 0.086; the dashed line represents p-tau/$A\beta_{42}$ cut-off 0.122. Bold lines represent comparisons with *p*-values < 0.05 at the Kruskal–Wallis

Table 2 Linear regression analyses, adjusted for age and sex, assessing the association between CSF amyloid biomarkers and CSF levels of p-tau

	A−T−		$CSFA\beta_{42}+$/amyR−		$CSFA\beta_{42}+$/amyR+		A+T+	
	β	*p*	*β*	*p*	*β*	*p*	*β*	*p*
$A\beta_{42}$	**.48**	**.003**	.10	.44	.12	.33	.16	.20
$A\beta_{40}$	**.58**	**<.001**	**.47**	**<.001**	**.48**	**<.001**	−0.07	.58
amyR	**−.33**	**.047**	**−.49**	**<.001**	**−.45**	**<.001**	.23	.08

Bold values represent *p*-value < 0.05

amyR $A\beta_{42}/A\beta_{40}$, *β* standardized coefficient, *p* *p*-value

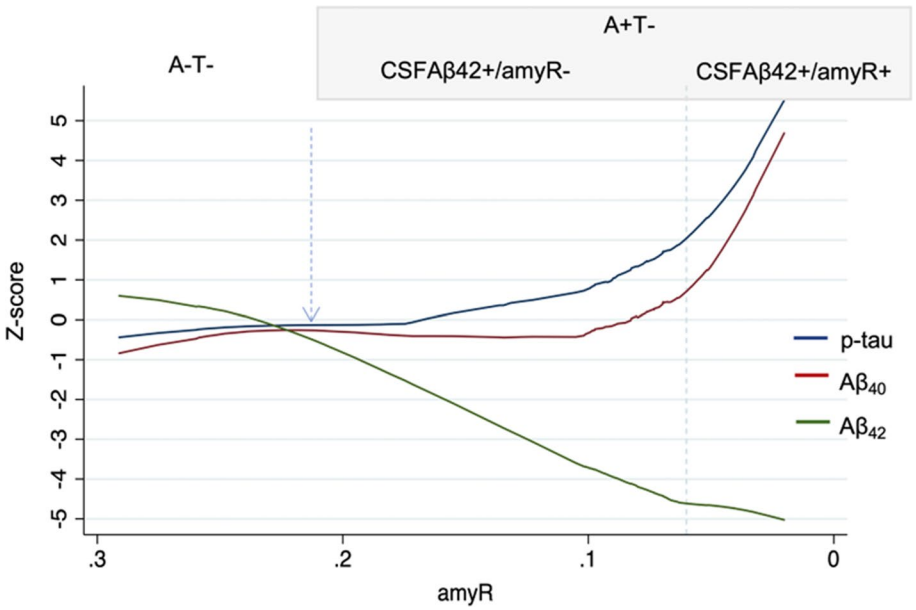

Fig. 2 Results of the robust locally weighted regression analysis showing changes of CSF biomarkers as a function of amyR. Values of *p*-tau, $A\beta_{42}$, and $A\beta_{40}$ are expressed as *z*-score standardized on the average and standard deviation of the A − T − group. The dotted line represents threshold value of pathological amyR (0.06), the dotted arrow indicates the point of change of $A\beta_{42}$ from normal to pathological values. CSF, cerebrospinal fluid; amyR, $A\beta_{42}/A\beta_{40}$; A, amyloid status; T, p-tau status)

chi-squared test to A + T − patients and found a different distribution of pathological p-tau/$A\beta_{42}$ levels between $CSFA\beta_{42}+$/amyR − and $CSFA\beta_{42}+$/amyR + subgroups [cut-off ≥ 0.086: 35.7% vs 78%, χ^2 (1, $n=105$) = 27.018, $p<0.001$; cut-off ≥ 0.122: 17.3% vs 63%, χ^2 (1, $n=105$) = 21.506, $p<0.001$].

In the logistic multivariate analyses, considering the variables age, sex, APOE E4 allele, hypertension, diabetes, and dyslipidemia, pathological amyR was significantly associated with a higher likelihood of having pathological p-tau/$A\beta_{42}$ [cut-off ≥ 0.086: OR 23.3 with a 95% CI of 4.0980–28.4627, $p<0.001$; cut-off ≥ 0.122: OR 8.8 with a 95% CI of 3.28–23.68, $p<0.001$] (Table 3). Nevertheless, some patients with normal amyR in the $CSFA\beta_{42}+$/amyR − group still showed pathological p-tau/$A\beta_{42}$ levels (cut-off ≥ 0.086: 35.7%; cut-off ≥ 0.122: 17.3%).

Table 3 Results of multivariate regression analysis exploring the odds of having pathological values of p-tau/$A\beta_{42}$ in A + T − patients

	p-tau/$A\beta_{42}$ cut-off ≥ 0.086		p-tau/$A\beta_{42}$ cut-off ≥ 0.122	
	Odds ratio (CI)	***p***	**Odds ratio (CI)**	***p***
amyR	23.27 (6.47–83.60)	**< 0.001**	8.82 (3.28–23.68)	**< 0.001**
Diabetes	0.38 (0.11–1.32)	0.13	0.51 (0.19–1.40)	0.19
Hypertension	0.99 (0.26–3.72)	0.99	1.25 (0.39–4.03)	0.71
Dyslipidemia	2.79 (0.71–10.95)	0.14	1.09 (0.34–3.47)	0.88
APOE4	5.93 (1.61–21.79)	**0.007**	1.27 (0.45–3.58)	0.65
Age	1.07 (0.99–1.14)	0.06	1.02 (0.96–1.07)	0.48
Sex	1.31 (0.43–4.03)	0.63	1.82 (0.68–4.91)	0.23

Bold values represent *p*-value < 0.05

amyR $A\beta_{42}/A\beta_{40}$, *CI* 95% confidence interval, *p p*-value

FDG-PET substudy

Demographics of the participants to the substudy are reported in Additional file 4. Two expert raters (A.M. and A.C.) separately evaluated FDG-PET scans from the 46 patients in the substudy and identified 37 typical AD patterns, four possible AD patterns, and five normal scans, showing good inter-rater agreement (Cohen's $k=0.9$). Holding scans with both typical and possible patterns as AD-positive, Cohen's *k* analysis demonstrated a significant agreement between abnormal FDG-PET and pathological CSF p-tau/$A\beta_{42}$ (Cohen's $k=0.73$), with a mismatch of 6% between them.

Comparisons between FDG-uptake patterns of each patient group versus CG showed a significant reduction in the temporo-parietal and frontal regions (see Additional file 5). The full factorial design, accounting for inter-group differences, resulted in a significant main effect of groups, and results from the post hoc analysis are shown in Table 4. Compared to the control

Table 4 Numerical results of SPM comparisons of FDG uptake in CG vs. CSFAβ_{42}+/amyR−, CSFAβ_{42}+/amyR− vs. CSFAβ_{42}+/amyR+, and CSFAβ_{42}+/amyR+ vs. A+T+

Analysis	Cluster level					Voxel level		
	Cluster *p* (FWE-corr)	Cluster *p* (FDR-corr)	Cluster extent	Cortical region	*Z* score of maximum	Talairach coordinates	Cortical region	BA
CG vs CSFAβ_{42}+/amyR−	0.000	0.000	31,175	L parietal lobe	Inf	−36, −74, 38	Precuneus	19
				L temporal lobe	Inf	−52, −56, −10	Middle temporal gyrus	37
				L parietal lobe	7.63	−48, −48, 44	Inferior parietal lobule	40
	0.001	0.000	1795	L frontal lobe	3.81	−26, 10, 58	Middle frontal gyrus	6
				L frontal lobe	3.61	−30, 26, 46	Middle frontal gyrus	8
				L frontal Lobe	3.43	−48, 30, 16	Inferior frontal gyrus	46
CSFAβ_{42}+/amyR− vs CSFAβ_{42}+/amyR+	0.000	0.000	6851	R frontal lobe	5.06	14, 62, 0	Medial frontal gyrus	10
				R frontal lobe	4.63	8, 60, 14	Medial frontal gyrus	10
				R limbic lobe	4.58	16, 32, 18	Anterior cingulate	32
CSFAβ_{42}+/amyR+ vs A+T+	n.s			n.a	n.a	n.a	n.a	n.a

In the "cluster level" section (left), the number of voxels, corrected *p*-value of significance, and cortical region where the voxel is found are all reported for each significant cluster. In the "voxel level" section, all the coordinates of the correlation sites (with the *Z*-score of the maximum correlation point), the corresponding cortical region and BA are reported for each significant cluster (CG, control group; Inf., infinite; L, left; R, right; BA, Brodmann area). When the maximum correlation is achieved outside the gray matter, the nearest gray matter (within a range of 5 mm) is indicated by the corresponding BA

group (CG), CSFAβ_{42}+/amyR− patients showed a significant reduction in brain glucose consumption in a wide cluster encompassing the left parietal (BAs 19 and 40), temporal (BA 37), and frontal lobes (BAs 6, 8, and 46) (Fig. 3A). With respect to CSFAβ_{42}+/amyR−, CSFAβ_{42}+/amyR+ showed an additional reduction in FDG uptake in the anterior regions, namely the anterior cingulate and frontomedial areas (BAs 32 and 10) (Fig. 3B). No differences were found between the hypometabolic patterns of CSFAβ_{42}+/amyR+ and A+T+ patients ($p > 0.05$).

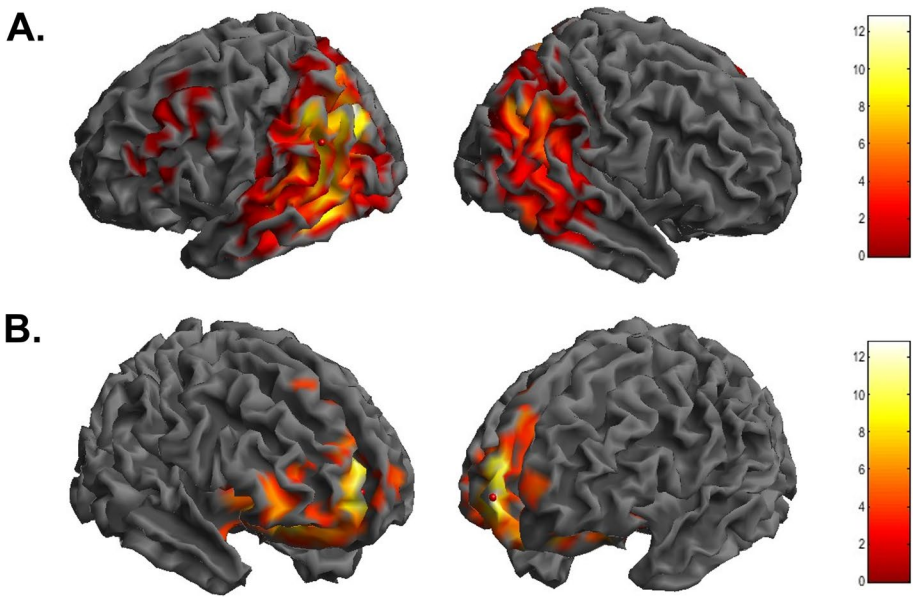

Fig. 3 3D brain rendering showing significant clusters obtained in SPM when comparing A−T− vs. CSFAβ_{42}+/amyR− (**A**) and CSFAβ_{42}+/amyR− vs. CSFAβ_{42}+/amyR+ (**B**). Color scale represents *t*-statistics values

Discussion

In the complex AD framework, the discordance between biomarkers, especially those accounting for amyloid status, might encourage both clinicians and researchers to prefer biomarkers with higher specificity, despite the risk of losing sensitivity and likely missing the problem of the different meanings associated with those biomarkers.

In the present study, we investigated whether $A\beta_{42}$ and amyR have different associations with AD-related burden, measured by CSF p-tau/$A\beta_{42}$ [2, 14, 20] and FDG-PET brain hypometabolism.

Main findings in CSF AD biomarkers and disease burden

CSF $A\beta_{42}$ levels did not significantly change across the AD continuum. Conversely, we identified a stepwise increase in CSF $A\beta_{40}$, with lower levels in controls as in CSF$A\beta_{42}+$/amyR−, higher levels in CSF$A\beta_{42}+$/amyR+, and the highest in A+T+, resembling the CSF variations of p-tau and p-tau/$A\beta_{42}$.

Decreased CSF $A\beta_{42}$ levels are a well-established finding in AD and could reflect the aggregation of $A\beta_{42}$ in brain tissue [27, 28], the formation of semisoluble $A\beta_{42}$ oligomers [29], or even the binding of peptides in complexes that mask epitopes targeted by analytical assays [30]. Moreover, the hypothetical temporal changes of AD biomarkers presume that the CSF $A\beta_{42}$ reduction begins in the pre-clinical stage [31]. However, repeated CSF measurements from symptomatic patients showed longitudinal stability of CSF $A\beta_{42}$ levels, making this biomarker unsuitable for reflecting the underlying dynamics of amyloid metabolism over time [32]. On the other hand, amyR is a better predictor of abnormal cortical amyloid plaque burden in AD [11, 12], possibly because the addition of CSF $A\beta_{40}$ in the ratio can correct for interindividual variability of amyloid production [33, 34]. However, another reasonable explanation may lie in a specific role of $A\beta_{40}$ in AD. Biochemical studies have shown that $A\beta_{42}$ has faster aggregation properties than other Aβ species and that $A\beta_{40}$ monomers inhibit its aggregation [35–37], by preferentially binding to protofibrillar $A\beta_{42}$ [38, 39]. Moreover, different ratios of $A\beta_{42}$ to $A\beta_{40}$ can result in different kinetics of amyloid fibrillization and aggregation. Chang and colleagues demonstrated that an equimolar $A\beta_{40}/A\beta_{42}$ sample generates oligomers with the highest neurotoxic effects on neuritic length, while an increase in the proportion of $A\beta_{40}$ stabilizes the fibrillization pathway [40]. However, an $A\beta_{40}$-dominant ratio causes changes in calcium dynamics, resulting in a higher elevation of intracellular calcium levels and neuronal apoptosis [41]. Thus, we may speculate that CSF levels of $A\beta_{40}$ initially increase to quench the fibrillization pathway triggered by $A\beta_{42}$ oligomerization; however, beyond a certain threshold, they may have toxic effects on neurons.

When we plotted the changes in CSF biomarkers as a function of amyR, we noticed different trends in CSF biomarkers variations. We observed that $A\beta_{42}$ had the steepest decrease before the amyR-positivity cut-off and then encountered a plateau phase. In contrast, CSF p-tau and $A\beta_{40}$ started increasing before the pathological threshold of amyR, but this increase was significantly more pronounced when amyR became pathological. This finding is consistent with the notion that cortical Aβ deposition precedes neocortical tau aggregation [34] and with previous studies reporting that the decrease in CSF $A\beta_{42}/A\beta_{40}$ ratio is followed by a large increase in CSF p-tau also in preclinical AD patients [42]. Indeed, we observed that a decrease of $A\beta_{42}$ in the CSF is accompanied by an increase of tau phosphorylation but also that the increase of $A\beta_{40}$ levels—which significantly affects amyR positivity—is accompanied by a steeper increase in CSF p-tau levels, which has recently been described to boost the spread of tau pathology in the brain [43].

In our cohort, we found that among A+T− patients, CSF$A\beta_{42}+$/amyR+ showed a higher probability of having pathological levels of p-tau/$A\beta_{42}$, a well-known marker of AD-related burden, than CSF$A\beta_{42}+$/amyR−. Considering the differences in CSF levels of $A\beta_{40,}$ but not $A\beta_{42}$, we might assume that the higher levels of $A\beta_{40}$ in CSF$A\beta_{42}+$/amyR+ could concur with these results.

Unexpectedly, although the CSF$A\beta_{42}+$/amyR− condition might be misinterpreted as an A− status if we relied on amyR more than CSF $A\beta_{42}$, in our study, we found that pathological values of p-tau/$A\beta_{42}$ can be present also in these patients. This highlights that amyR, commonly held as the best biomarker for detecting amyloid pathology [35], also shows suboptimal negative predictive power, suggesting that the added value of $A\beta_{40}$ could lie beyond its $A\beta_{42}$-corrective function, since correcting for interindividual amyloid production variability should improve not only amyR specificity but also sensitivity.

The specific meaning of the altered CSF $A\beta_{40}$ levels could be rooted in its significant correlation with the CSF levels of p-tau, which is also present under physiological conditions [44]. In our results, we observed a positive linear relationship between $A\beta_{40}$ and p-tau in A−T−, CSF$A\beta_{42}+$/amyR−, and CSF$A\beta_{42}+$/amyR+, but not in A+T+. We cannot exclude that, alongside pathological $A\beta_{42}$ levels, there may be a concomitant increase in CSF $A\beta_{40}$ (as in CSF$A\beta_{42}+$/amyR+ patients) associated with a parallel increase in tau phosphorylation. Conversely, in our A+T+ group tau pathology seems to proceed independently from amyloid pathology as no association was found between amyloid and tau CSF biomarkers. In line with our results, it has been recently demonstrated that

the Aβ-induced increase in CSF p-tau levels might play a key role in initiating tau aggregation and spreading in early AD, while local tau seeding and auto-replication predominate once soluble p-tau concentrations reach a plateau in AD dementia [43].

Main findings in FDG-PET metabolic pattern

To support our hypothesis that CSFAβ_{42}+and amyR+hold different meanings in AD pathophysiology, we considered patterns of brain glucose metabolism. Indeed, specific FDG-PET hypometabolic patterns have been demonstrated to predict AD dementia [15–17] and may detect additional differences between CSFAβ_{42}+/amyR−and CSFAβ_{42}+/amyR+.

First, when comparing FDG-PET scans from CSFAβ_{42}+/amyR−patients and controls, we found a pattern of cortical hypometabolism encompassing the parietal and frontotemporal regions. Thus, the decrease in CSF Aβ_{42} alone may be associated with synaptic dysfunction and reduced brain glucose uptake in areas typically involved in AD [45, 46]. However, other crucial factors (i.e., such as endothelial dysfunction, neuroinflammation, and astrocytic impairment) could also have influenced synaptic functioning, especially in the very early stages of the disease, before overt amyloid pathology occurs [47–49].

In contrast, patients with CSFAβ_{42}+/amyR+showed further involvement of the frontal regions, configuring an FDG-PET pattern indistinguishable from A+T+. Previous studies have shown that soluble Aβ_{40}, but not Aβ_{42}, extracted from the frontal cortex of patients with AD gradually increases along with the progression of Braak scores, suggesting a specific link between Aβ_{40} levels and the progression of tau pathology [50]. Moreover, a positive correlation between soluble tau levels and hypometabolism in the frontal regions has also been reported [51]. Our findings suggest that amyR positivity, which in our cohort is determined by the co-presence of decreased Aβ_{42} and increased Aβ_{40} levels, is associated with widespread brain hypometabolism, and probably with the spread of tau pathology, even in the absence of elevated tau proteins in the CSF [52].

The lack of detection of elevated levels of CSF p-tau$_{181}$ in our cohort does not exclude a possible increase of other p-tau isoforms (e.g., p-tau$_{217}$ or p-tau$_{231}$). Moreover, a threshold-based evaluation of CSF p-tau, as for other fluid biomarkers, can have limitations tied to the risk of false negative results, whose occurrence also encompasses pre-analytical (e.g., collection techniques, handling of samples, storage conditions) and analytical variables (e.g., accuracy in sample processing, assay sensitivity) [53]. On the other hand, there may be other yet-to-be elucidated pathophysiological processes underlying a possible mismatch between parenchymal and CSF evidence of tau pathology. Considering all these limitations, a multimodal approach combining imaging and CSF biomarkers could be advisable.

Our results show that among patients classified as A+T−, there is a group with reduced Aβ_{42} and low Aβ_{40} (CSFAβ_{42}+/amyR−) that differ from healthy controls for showing typical AD patterns of cerebral hypometabolism, and a second group with reduced Aβ_{42} and high Aβ_{40} (CSFAβ_{42}+/amyR+) showing widespread reduction of brain glucose uptake, undistinguishable from biologically defined AD patients (A+T+).

Limitations

To our knowledge, this study is the first to directly compare CSFAβ_{42}+/amyR−and CSFAβ_{42}+/amyR+patients, as well as the first to examine differences and overlap between them, healthy controls, and A+T+in terms of CSF p-tau, AD-related burden, and brain FDG-PET metabolic patterns. However, because of its cross-sectional design, we could not investigate temporal connection between different biomarkers alteration or evaluate whether higher CSF Aβ_{40} levels, along with pathological CSF Aβ_{42}, may affect the rapidity of cognitive decline.

Furthermore, fluid biomarkers, represented on a continuous scale, are commonly used in a dichotomous way, applying cut-offs whose thresholds become crucial in clinical practice. Such thresholds are not always available for every biomarker measure, and a global effort of standardization is needed to increase accuracy and reproducibility of these findings. Further investigations using amyloid-PET or tau-PET would be useful to verify our results on the prevalence of pathological AD-related burden across patient groups—which we evaluated indirectly via the CSF p-tau/Aβ_{42} ratio—and to assess any causal connections between the alteration of Aβ_{42}, Aβ_{40}, and p-tau in the CSF and parenchymal amyloid and tau deposition. Finally, extending the analysis by comparing blood-based and CSF biomarkers could be useful to confirm these relationships and to assess their extensibility for diagnostic and prognostic purposes.

Conclusions

Fluid biomarkers are nowadays being introduced into clinical routine practice, positing challenges on their correct use for either supporting or excluding AD diagnosis.

Patients with cognitive symptoms and decreased CSF Aβ_{42} without pathological amyR nor increased p-tau levels could, under certain circumstances, be essentially considered non-AD, but this conclusion can be hard to reach when clinical presentation and FDG-PET pattern are highly suggestive of AD. Our results suggest that decreased CSF Aβ_{42} alone could detect Alzheimer's pathology, since these patients are distinguished

from controls by reduced FDG uptake in brain regions typical of AD, and some of them also show pathological measures of AD-related burden.

On the other hand, the increase in CSF $A\beta_{40}$ levels, traced by pathological amyR, associates with higher levels of soluble hyperphosphorylated tau, higher AD-related burden, and a widespread pattern of FDG hypometabolism.

Considering the many experimental novel drugs that see Aβ and tau proteins as therapeutic targets, the specific meaning of different amyloid CSF biomarkers should be considered to support a more accurate selection of patients and search for the best time window for treatment.

Abbreviations

AD	Alzheimer's disease
Aβ	Amyloid-β
amyR	Amyloid ratio
BA	Brodmann area
CSF	Cerebrospinal fluid
CT	Computed tomography
FDG	Fludeoxyglucose
MRI	Magnetic resonance imaging
MMSE	Mini-Mental State Examination
PET	Positron emission tomography
PCR	Polymerase chain reaction
SPM	Statistical parametric mapping

Supplementary Information

The online version contains supplementary material available at https://doi.org/10.1186/s13195-023-01291-w.

Additional file 1. Flowcharts summarizing patients' enrolment (A) and control group selection (B) procedures for the CSF study.

Additional file 2. Flowcharts summarizing patients' enrolment (A) and control group selection (B) procedures for the FDG-PET substudy.

Additional file 3. Scatter Plots showing correlations (Spearman's rho) between CSF p-tau and different amyloid biomarkers ($A\beta_{42}$, $A\beta_{40}$, amyR) in A-T-, CSF$A\beta_{42}$+/amyR-, CSF$A\beta_{42}$+/amyR+ and A+T+.

Additional file 4. Demographical, clinical and biomarkers data from FDG-PET substudy.

Additional file 5. Numerical results of SPM comparisons of FDG uptake in CG vs. CSFAβ42+/amyR-, CG vs. CSFAβ42+/amyR+ and CG vs. A+T+.

Acknowledgements
None.

Authors' contributions
CM and AM conceptualized the study and revised the manuscript. CM, MDD, CGB and AC analyzed and interpreted the data, drafted and revised the manuscript, did the statistical analysis, and prepared the figures. MA, NBM and GK participated in the interpretation of the data and revision of the manuscript.

Funding
This study was not supported by any grant.

Availability of data and materials
The dataset analyzed in this study is available from the corresponding author upon reasonable request.

Declarations

Ethics approval and consent to participate
All participants or legal representatives signed a written informed consent for the anonymization, storage, and analysis of all clinical and biological data. The local ethics committee approved this protocol as an observational retrospective study, which was conducted according to the Declaration of Helsinki.

Consent for publication
Not applicable.

Competing interests
The authors declare no competing interests.

Author details
[1]UOSD Centro Demenze, University of Rome "Tor Vergata", Rome, Italy. [2]Experimental Neuropsychophysiology Laboratory, IRCCS Santa Lucia Foundation, Rome, Italy. [3]Department of Biomedicine and Prevention, University of Rome Tor Vergata, Rome, Italy. [4]Istituto Neurologico Mediterraneo, Pozzilli, Italy. [5]Human Physiology Unit, Department of Neuroscience and Rehabilitation, University of Ferrara, Ferrara, Italy.

Received: 25 May 2023 Accepted: 18 August 2023
Published online: 30 August 2023

References

1. Jack CR, Bennett DA, Blennow K, et al. NIA-AA research framework: toward a biological definition of Alzheimer's disease. Alzheimer's Dement. 2018;14(4):535–62. https://doi.org/10.1016/j.jalz.2018.02.018.
2. Tapiola T, Alafuzoff I, Herukka SK, et al. Cerebrospinal fluid {beta}-amyloid 42 and tau proteins as biomarkers of Alzheimer-type pathologic changes in the brain. Arch Neurol. 2009;66(3):382–9. https://doi.org/10.1001/ARCHNEUROL.2008.596.
3. Long JM, Coble DW, Xiong C, et al. Preclinical Alzheimer's disease biomarkers accurately predict cognitive and neuropathological outcomes. 2022. https://doi.org/10.1093/brain/awac250.
4. Baldeiras I, Santana I, Leitão MJ, et al. Addition of the Aβ42/40 ratio to the cerebrospinal fluid biomarker profile increases the predictive value for underlying Alzheimer's disease dementia in mild cognitive impairment. Alzheimers Res Ther. 2018;10(1). https://doi.org/10.1186/S13195-018-0362-2.
5. Slaets S, Le Bastard N, Martin JJ, et al. Cerebrospinal fluid Aβ1-40 improves differential dementia diagnosis in patients with intermediate P-tau181P levels. J Alzheimers Dis. 2013;36(4):759–67. https://doi.org/10.3233/JAD-130107.
6. Sauvée M, DidierLaurent G, Latarche C, Escanyé M-C, Olivier J-L, Malaplate-Armand C. Additional use of Aβ 42/Aβ 40 ratio with cerebrospinal fluid biomarkers P-Tau and Aβ 42 increases the level of evidence of Alzheimer's disease pathophysiological process in routine practice. J Alzheimer's Dis. 2014;41(2):377–86. https://doi.org/10.3233/JAD-131838.
7. Dorey A, Perret-Liaudet A, Tholance Y, Fourier A, Quadrio I. Cerebrospinal fluid Aβ40 improves the interpretation of Aβ42 concentration for diagnosing Alzheimer's disease. Front Neurol. 2015;6(NOV). https://doi.org/10.3389/FNEUR.2015.00247.
8. Dumurgier J, Schraen S, Gabelle A, et al. Cerebrospinal fluid amyloid-β 42/40 ratio in clinical setting of memory centers: a multicentric study. Alzheimers Res Ther. 2015;7(1). https://doi.org/10.1186/S13195-015-0114-5.
9. Niemantsverdriet E, Ottoy J, Somers C, et al. The cerebrospinal fluid Aβ1-42/Aβ1-40 ratio improves concordance with amyloid-PET for diagnosing Alzheimer's disease in a clinical setting. J Alzheimers Dis. 2017;60(2):561–76. https://doi.org/10.3233/JAD-170327.
10. Amft M, Ortner M, Eichenlaub U, et al. The cerebrospinal fluid biomarker ratio Aβ42/40 identifies amyloid positron emission tomography positivity better than Aβ42 alone in a heterogeneous memory clinic cohort. Alzheimer's Res Ther. 2022;14(1):1–9. https://doi.org/10.1186/S13195-022-01003-W/FIGURES/2.
11. Janelidze S, Pannee J, Mikulskis A, et al. Concordance between different amyloid immunoassays and visual amyloid positron emission tomographic assessment. JAMA Neurol. 2017;74(12):1492–501. https://doi.org/10.1001/JAMANEUROL.2017.2814.

12. Lewczuk P, Mroczko B, Fagan A, Kornhuber J. Biomarkers of Alzheimer's disease and mild cognitive impairment: a current perspective. Adv Med Sci. 2015;60(1):76–82. https://doi.org/10.1016/J.ADVMS.2014.11.002.
13. Vromen EM, de Boer SCM, Teunissen CE, et al. Biomarker A+T-: is this Alzheimer's disease or not? A combined CSF and pathology study. Brain. 2022. https://doi.org/10.1093/BRAIN/AWAC158.
14. Maddalena A, Papassotiropoulos A, Müller-Tillmanns B, et al. Biochemical diagnosis of Alzheimer disease by measuring the cerebrospinal fluid ratio of phosphorylated tau protein to beta-amyloid peptide42. Arch Neurol. 2003;60(9):1202–6. https://doi.org/10.1001/ARCHNEUR.60.9.1202.
15. Perani D, Cerami C, Caminiti SP, et al. Cross-validation of biomarkers for the early differential diagnosis and prognosis of dementia in a clinical setting. Eur J Nucl Med Mol Imaging. 2016;43(3):499–508. https://doi.org/10.1007/S00259-015-3170-Y.
16. Caminiti SP, Ballarini T, Sala A, et al. FDG-PET and CSF biomarker accuracy in prediction of conversion to different dementias in a large multicentre MCI cohort. NeuroImage Clin. 2018;18:167–77. https://doi.org/10.1016/J.NICL.2018.01.019.
17. Inui Y, Ito K, Kato T. Longer-term investigation of the value of 18F-FDG-PET and magnetic resonance imaging for predicting the conversion of mild cognitive impairment to Alzheimer's disease: a multicenter study. J Alzheimers Dis. 2017;60(3):877–87. https://doi.org/10.3233/JAD-170395.
18. McKhann GM, Knopman DS, Chertkow H, et al. The diagnosis of dementia due to Alzheimer's disease: recommendations from the National Institute on Aging-Alzheimer's Association workgroups on diagnostic guidelines for Alzheimer's disease. Alzheimer's Dement. 2011;7(3):263–9. https://doi.org/10.1016/j.jalz.2011.03.005.
19. Albert MS, DeKosky ST, Dickson D, et al. The diagnosis of mild cognitive impairment due to Alzheimer's disease: recommendations from the National Institute on Aging-Alzheimer's Association workgroups on diagnostic guidelines for Alzheimer's disease. Alzheimer's Dement. 2011;7(3):270–9. https://doi.org/10.1016/j.jalz.2011.03.008.
20. Constantinides VC, Paraskevas GP, Boufidou F, et al. CSF Aβ42 and Aβ42/Aβ40 ratio in Alzheimer's disease and frontotemporal dementias. Diagnostics. 2023;13(4):783. https://doi.org/10.3390/DIAGNOSTICS13040783.
21. Cleveland WS. Robust locally weighted regression and smoothing scatterplots. J Am Stat Assoc. 1979;74(368):829–36. https://doi.org/10.1080/01621459.1979.10481038.
22. Guedj E, Varrone A, Boellaard R, et al. EANM procedure guidelines for brain PET imaging using [18F]FDG, version 3. Eur J Nucl Med Mol Imaging. 2022;49(2):632–51. https://doi.org/10.1007/S00259-021-05603-W.
23. D'Agostino E, Maes F, Vandermeulen D, Suetens P. Atlas-to-image non-rigid registration by minimization of conditional local entropy. Lect Notes Comput Sci (including Subser Lect Notes Artif Intell Lect Notes Bioinformatics). 2007;4584 LNCS:320–332. https://doi.org/10.1007/978-3-540-73273-0_27/COVER.
24. Mazziotta JC, Toga AW, Evans A, Fox P, Lancaster J. A probabilistic atlas of the human brain: theory and rationale for its development. Neuroimage. 1995;2(2):89–101. https://doi.org/10.1006/nimg.1995.1012.
25. Mazziotta J, Toga A, Evans A, et al. A four-dimensional probabilistic atlas of the human brain. J Am Med Inform Assoc. 2001;8(5):401. https://doi.org/10.1136/JAMIA.2001.0080401.
26. Bennett CM, Wolford GL, Miller MB. The principled control of false positives in neuroimaging. Soc Cogn Affect Neurosci. 2009;4(4):417–22. https://doi.org/10.1093/SCAN/NSP053.
27. Strozyk D, Blennow K, White LR, Launer LJ. CSF Aß 42 levels correlate with amyloid-neuropathology in a population-based autopsy study. Neurology. 2003;60(4):652–6. https://doi.org/10.1212/01.WNL.0000046581.81650.D0.
28. Fagan AM, Mintun MA, Mach RH, et al. Inverse relation between in vivo amyloid imaging load and cerebrospinal fluid Abeta42 in humans. Ann Neurol. 2006;59(3):512–9. https://doi.org/10.1002/ANA.20730.
29. Walsh DM, Klyubin I, Shankar GM, et al. The role of cell-derived oligomers of Aβ in Alzheimer's disease and avenues for therapeutic intervention. Biochem Soc Trans. 2005;33(5):1087–90. https://doi.org/10.1042/BST20051087.
30. Bjerke M, Portelius E, Minthon L, et al. Confounding factors influencing amyloid beta concentration in cerebrospinal fluid. Int J Alzheimers Dis Published online. 2010. https://doi.org/10.4061/2010/986310.
31. Stomrud E, Minthon L, Zetterberg H, Blennow K, Hansson O. Longitudinal cerebrospinal fluid biomarker measurements in preclinical sporadic Alzheimer's disease: a prospective 9-year study. Alzheimer's Dement Diagnosis, Assess Dis Monit. 2015;1(4):403–11. https://doi.org/10.1016/j.dadm.2015.09.002.
32. Le Bastard N, Aerts L, Sleegers K, et al. Longitudinal stability of cerebrospinal fluid biomarker levels: fulfilled requirement for pharmacodynamic markers in Alzheimer's disease. J Alzheimers Dis. 2013;33(3):807–22. https://doi.org/10.3233/JAD-2012-110029.
33. Biscetti L, Salvadori N, Farotti L, et al. The added value of Aβ42/Aβ40 in the CSF signature for routine diagnostics of Alzheimer's disease. Clin Chim Acta. 2019;494:71–3. https://doi.org/10.1016/J.CCA.2019.03.001.
34. Hansson O, Lehmann S, Otto M, Zetterberg H, Lewczuk P. Advantages and disadvantages of the use of the CSF Amyloid β (Aβ) 42/40 ratio in the diagnosis of Alzheimer's disease. Alzheimers Res Ther. 2019;11(1):1–15. https://doi.org/10.1186/S13195-019-0485-0.
35. Murray MM, Bernstein SL, Nyugen V, Condron MM, Teplow DB, Bowers MT. Amyloid protein: A40 inhibits A42 oligomerization. 2009;131(18):6136–6137. https://doi.org/10.1021/ja8092604.
36. Jan A, Gokce O, Luthi-Carter R, Lashuel HA. The ratio of monomeric to aggregated forms of Abeta40 and Abeta42 is an important determinant of amyloid-beta aggregation, fibrillogenesis, and toxicity. J Biol Chem. 2008;283(42):28176–89. https://doi.org/10.1074/JBC.M803159200.
37. Hasegawa K, Yamaguchi I, Omata S, Gejyo F, Naiki H. Interaction between A beta(1–42) and A beta(1–40) in Alzheimer's beta-amyloid fibril formation in vitro. Biochemistry. 1999;38(47):15514–21. https://doi.org/10.1021/BI991161M.
38. Yan Y, Wang C. Abeta40 protects non-toxic Abeta42 monomer from aggregation. J Mol Biol. 2007;369(4):909–16. https://doi.org/10.1016/J.JMB.2007.04.014.
39. Pauwels K, Williams TL, Morris KL, et al. Structural basis for increased toxicity of pathological aβ42:aβ40 ratios in Alzheimer disease. J Biol Chem. 2012;287(8):5650–60. https://doi.org/10.1074/JBC.M111.264473.
40. Kuperstein I, Broersen K, Benilova I, et al. Neurotoxicity of Alzheimer's disease Aβ peptides is induced by small changes in the Aβ42 to Aβ40 ratio. EMBO J. 2010;29(19):3408–20. https://doi.org/10.1038/EMBOJ.2010.211.
41. Chang YJ, Chen YR. The coexistence of an equal amount of Alzheimer's amyloid-β 40 and 42 forms structurally stable and toxic oligomers through a distinct pathway. FEBS J. 2014;281(11):2674–87. https://doi.org/10.1111/FEBS.12813.
42. Milà-Alomà M, Salvadó G, Gispert JD, et al. Amyloid beta, tau, synaptic, neurodegeneration, and glial biomarkers in the preclinical stage of the Alzheimer's continuum. Alzheimers Dement. 2020;16(10):1358–71. https://doi.org/10.1002/ALZ.12131.
43. Pichet Binette A, Franzmeier N, Spotorno N, et al. Amyloid-associated increases in soluble tau relate to tau aggregation rates and cognitive decline in early Alzheimer's disease. Nat Commun. 2022;13(1):6635. https://doi.org/10.1038/S41467-022-34129-4.
44. Lehmann S, Dumurgier J, Ayrignac X, et al. Cerebrospinal fluid A beta 1–40 peptides increase in Alzheimer's disease and are highly correlated with phospho-tau in control individuals. Alzheimers Res Ther. 2020;12(1). https://doi.org/10.1186/S13195-020-00696-1.
45. Nobili F, Arbizu J, Bouwman F, et al. European Association of Nuclear Medicine and European Academy of Neurology recommendations for the use of brain 18 F-fluorodeoxyglucose positron emission tomography in neurodegenerative cognitive impairment and dementia: Delphi consensus. Eur J Neurol. 2018;25(10):1201–17. https://doi.org/10.1111/ENE.13728.
46. Minoshima S, Cross D, Thientunyakit T, Foster NL, Drzezga A. 18F-FDG PET imaging in neurodegenerative dementing disorders: insights into subtype classification, emerging disease categories, and mixed dementia with copathologies. J Nucl Med. 2022;63(Suppl 1):2S-12S. https://doi.org/10.2967/JNUMED.121.263194.
47. Salvadó G, Shekari M, Falcon C, et al. Brain alterations in the early Alzheimer's continuum with amyloid-β, tau, glial and neurodegeneration CSF markers. Brain Commun. 2022;4(3). https://doi.org/10.1093/BRAINCOMMS/FCAC134.
48. Tubi MA, Kothapalli D, Hapenney M, et al. Regional relationships between CSF VEGF levels and Alzheimer's disease brain biomarkers and cognition. Neurobiol Aging. 2021;105:241–51. https://doi.org/10.1016/J.NEUROBIOLAGING.2021.04.025.
49. Bonomi CG, Chiaravalloti A, Camedda R, et al. Functional correlates of microglial and astrocytic activity in symptomatic sporadic Alzheimer's disease: a CSF/18F-FDG-PET study. Biomed. 2023;11(3):725. https://doi.org/10.3390/BIOMEDICINES11030725.

50. Thorwald MA, Silva J, Head E, Finch CE. Amyloid futures in the expanding pathology of brain aging and dementia. Alzheimer's Dement. 2023;19(6):2605–17. https://doi.org/10.1002/ALZ.12896.
51. Chiaravalloti A, Barbagallo G, Ricci M, et al. Brain metabolic correlates of CSF Tau protein in a large cohort of Alzheimer's disease patients: A CSF and FDG PET study. Brain Res. 2018;1678:116–22. https://doi.org/10.1016/J.BRAINRES.2017.10.016.
52. Tijms BM, Gobom J, Reus L, et al. Pathophysiological subtypes of Alzheimer's disease based on cerebrospinal fluid proteomics. Brain. 2020;143(12):3776–92. https://doi.org/10.1093/BRAIN/AWAA325.
53. Fourier A, Portelius E, Zetterberg H, Blennow K, Quadrio I, Perret-Liaudet A. Pre-analytical and analytical factors influencing Alzheimer's disease cerebrospinal fluid biomarker variability. Clin Chim Acta. 2015;449:9–15. https://doi.org/10.1016/J.CCA.2015.05.024.

Publisher's Note